



## Effects of caloric restriction and ketogenic diet on renal fibrosis after ischemia/reperfusion injury

E.I. Yakupova<sup>a,\*\*</sup>, D.S. Semenov<sup>a</sup>, P.A. Abramicheva<sup>a</sup>, L.D. Zorova<sup>a,b</sup>, I.B. Pevzner<sup>a,b</sup>, N.V. Andrianova<sup>a</sup>, V.A. Popkov<sup>a,b</sup>, V.N. Mansikh<sup>a</sup>, A.D. Bocharnikov<sup>c</sup>, Y.A. Voronina<sup>d,e</sup>, D.B. Zorov<sup>a,b</sup>, E.Y. Plotnikov<sup>a,b,\*</sup>

<sup>a</sup> A.N. Belozersky Institute of Physico-Chemical Biology, Lomonosov Moscow State University, Moscow 119234, Russia

<sup>b</sup> V.I. Kulakov National Medical Research Center of Obstetrics, Gynecology, and Perinatology, Moscow 117997, Russia

<sup>c</sup> Sechenov First Moscow State Medical University, Moscow 119992, Russia

<sup>d</sup> Department of Human and Animal Physiology, Lomonosov Moscow State University, Moscow 119234, Russia

<sup>e</sup> Laboratory of Cardiac Electrophysiology, National Medical Research Center for Cardiology, Moscow 121552, Russia

### ARTICLE INFO

#### Keywords:

Caloric restriction  
Ketogenic diet  
Kidney fibrosis  
Ischemia/reperfusion injury  
Glycolysis  
Krebs cycle

### ABSTRACT

The beneficial effects of caloric restriction (CR) and a ketogenic diet (KD) have been previously shown when performed prior to kidney injury. We investigated the effects of CR and KD on fibrosis development after unilateral kidney ischemia/reperfusion (UIR). Post-treatment with CR significantly ( $p < 0.05$ ) affected blood glucose (2-fold decrease), ketone bodies (3-fold increase), lactate (1.5-fold decrease), and lipids (1.4-fold decrease). In the kidney, CR improved succinate dehydrogenase and malate dehydrogenase activity by 2-fold each, but worsened fibrosis progression. Similar results were shown for the KD, which restored the post-UIR impaired activities of succinate dehydrogenase, malate dehydrogenase, and  $\alpha$ -ketoglutarate dehydrogenase (which was decreased 2-fold) but had no effect on fibrosis progression. Thus, our study shows that the use of CR or KD after UIR did not reduce the development of fibrosis, as shown by hydroxyproline content, western-blotting, and RT-PCR, whereas it caused significant metabolic changes in kidney tissue after UIR.

### 1. Introduction

The transition from acute kidney injury (AKI) to chronic kidney disease (CKD) is accompanied by the appearance of scar tissue (fibrosis) [1], which impairs renal function and can be fatal [2]. Fibrosis in various organs is known to be responsible for nearly 45 % of deaths in developed countries [3]. The incidence of CKD and kidney fibrosis has steadily increased since the 1990s, and 1.2 million people died of CKD worldwide in 2017 [4]. Given the prevalence and dangerous nature of renal fibrosis, the search for antifibrotic drugs and treatment strategies is urgent.

Fibrosis formation may be associated with changes in cell bioenergetics. For instance, glycolytic flux may be a critical point in the regulation of collagen synthesis and fibrosis development in various pathologies [5]. Retardation of certain glycolytic enzymes leads to a decrease in fibrosis development in various organs, which has been demonstrated in both cell and animal models. On the other hand,

\* Corresponding author. A.N. Belozersky Institute of Physico-Chemical Biology, Lomonosov Moscow State University, Moscow 119234, Russia.

\*\* Corresponding author.

E-mail addresses: [elmira.yaku@gmail.com](mailto:elmira.yaku@gmail.com) (E.I. Yakupova), [plotnikov@belozersky.msu.ru](mailto:plotnikov@belozersky.msu.ru) (E.Y. Plotnikov).

<https://doi.org/10.1016/j.heliyon.2023.e21003>

Received 10 May 2023; Received in revised form 25 September 2023; Accepted 12 October 2023

Available online 16 October 2023

2405-8440/© 2023 The Authors. Published by Elsevier Ltd. This is an open access article under the CC BY-NC-ND license (<http://creativecommons.org/licenses/by-nc-nd/4.0/>).

suppression of the fatty acid oxidation pathway results in an increase in the synthesis of extracellular matrix (ECM) proteins even when glycolytic activity remains unchanged [5].

The ECM is a crucial element of tissue architecture necessary to give the organ its proper shape and to perform a number of other functions: in particular, transport, signaling, etc. Excessive formation of EMC is found in a number of pathological processes and is often associated with inflammation. Turnover of ECM elements is a largely energy-dependent process and energy metabolism is important for maintaining ECM homeostasis. Therefore, approaches affecting metabolism may be a promising strategy to manage and reduce fibrosis. This requires in-depth experimental investigation [5,6].

Dietary approaches, especially caloric restriction (CR), have previously been shown to be protective in the treatment of various pathological processes [7–12], including AKI [12,13]. Moreover, the protective properties of fasting against the development of tubulointerstitial fibrosis have been previously demonstrated [14]. In further studies, researchers have shown that fasting affords protection against renal injury and fibrosis development associated with ischemia-induced AKI [15].

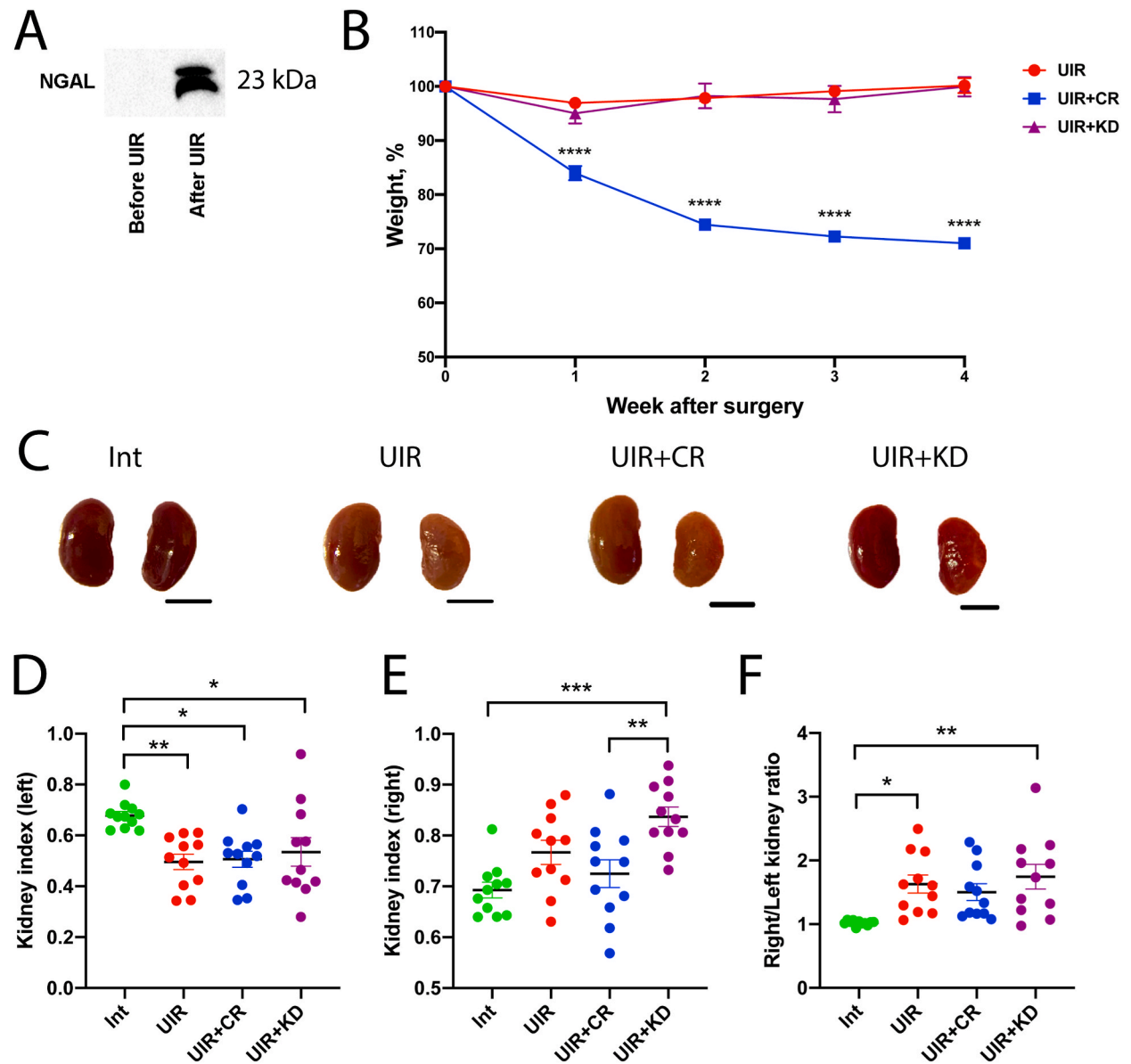


**Fig. 1.** Morphology and weight changes in mice and their kidneys after UIR. (A) Detection of NGAL in urine samples before and 24 h after surgery by Western blotting. The uncropped images are available in the supplementary material of the manuscript (S1). (B) Dynamics of body weight during 4 weeks after UIR of the experiment in mice fed different diets (\*\*\*\* $p < 0.0001$  in UIR and UIR + CR differences (T-test and Mann-Whitney  $U$  test). (C) Appearance of intact right and ischemic left kidney 4 weeks after UIR (bar, 5 mm) when exposed to different feeding protocols. (D) Left kidney index. (E) Right kidney index. (F) Ratio of kidney weights. For all groups,  $n = 11$ .

KD has been shown to attenuate acute and chronic ischemic kidney injury and reduce markers of oxidative stress and inflammation [16]. On the other hand, feeding a ketogenic diet (KD) for 4 weeks impaired interstitial fibrosis and exacerbated cardiac remodeling in spontaneously hypertensive rats [17]. After exogenous administration of  $\beta$ -hydroxybutyrate ( $\beta$ -OHB) mimicking KD, a decrease in mitochondrial biogenesis and an increase in cardiac fibrosis were demonstrated in rats [17]. Therefore, further studies are needed to uncover the relationship between dietary approaches and fibrosis formation before they can be used in humans.

Note that in most studies, diets were performed prior to onset of AKI. Therefore, in this work, we investigated how KD or CR affected the development of kidney fibrosis when used after unilateral kidney ischemia/reperfusion (UIR).

## 2. Results

To diagnose AKI after UIR, we examined urinary neutrophil gelatinase-associated lipocalin (NGAL) levels. NGAL was not detected in urine samples collected before UIR, but this marker protein increased one day after surgery (Fig. 1A), indicating the development of AKI.

Weekly body weight dynamics showed that mice fed 35 % CR lost approximately 30 % of their weight by the end of week 4 ( $p = 0.0001$ ), while mice fed KD had the same weight as *ad libitum* fed mice (Fig. 1B). At 4 week post-UIR, left kidneys exposed to ischemia appeared smaller than intact (Int) right kidneys and had a rough surface (Fig. 1C). In addition to visual assessment, we measured kidney index for the left and right kidneys (Fig. 1D and E) and the weight ratio of the kidneys (Fig. 1F), indicating irreversible tissue loss after kidney injury. In general, UIR resulted in a significant 1.2-fold decrease in left kidney index in all groups ( $p < 0.05$  for UIR +

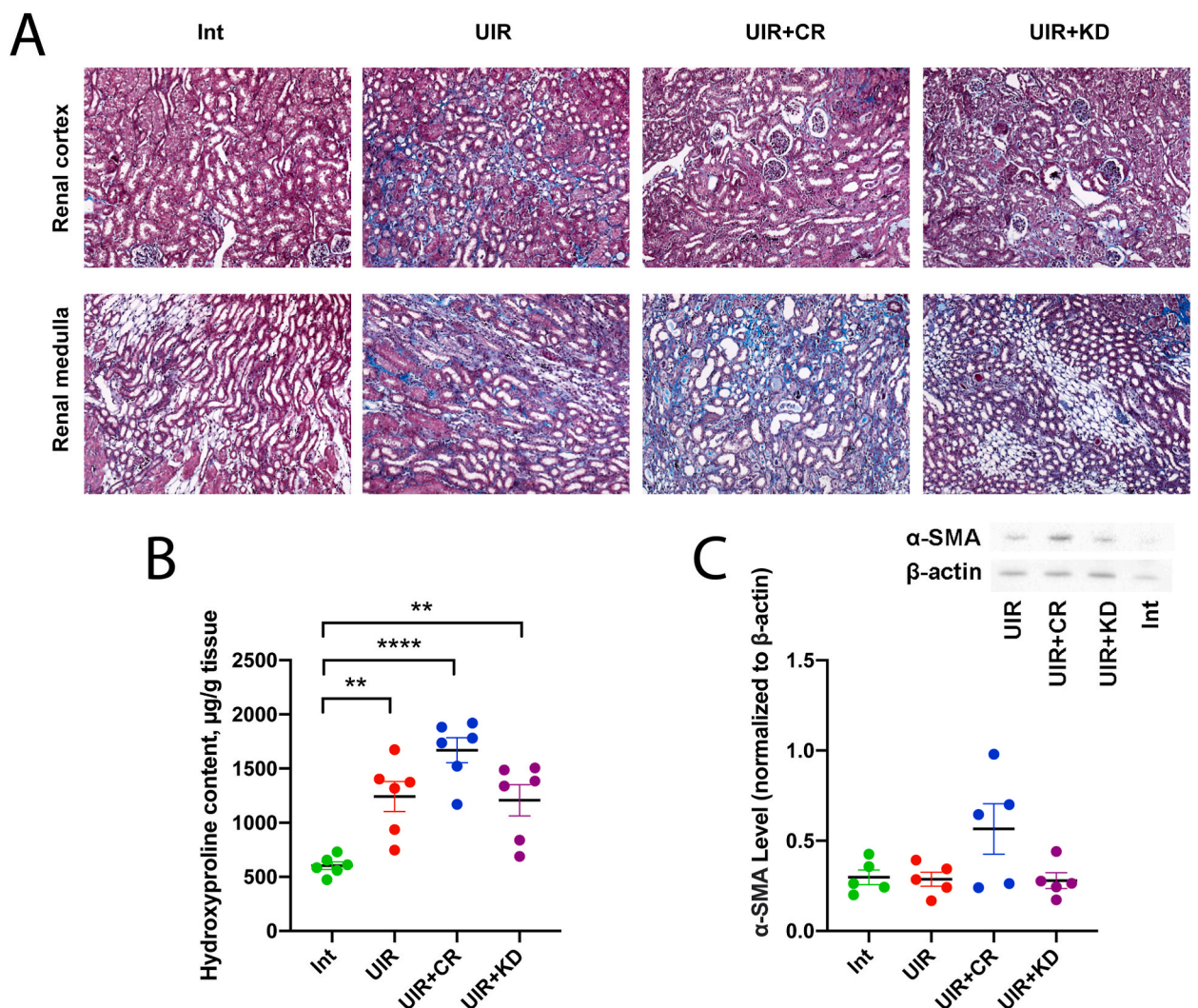


**Fig. 2.** Analysis of renal fibrosis. (A) Kidneys were stained with Masson trichrome to identify collagen deposition. (B) Changes in Hyp concentration after hydrolysis of kidney tissue ( $n = 6$ ). (C) Western blot analysis of  $\alpha$ -SMA levels in kidneys ( $n = 5$ ). The uncropped images are available in the supplementary material of the manuscript (Fig. S2).

CR and KD,  $p < 0.005$  for UIR compared to Int control) (Fig. 1D) and to some increase in the right kidney index (Fig. 1E): by 1.2-fold in the case of UIR + KD ( $p < 0.0005$ ), which ultimately translated into an increased right-to-left kidney ratio (Fig. 1F). In the UIR + KD group, these changes were significant ( $p < 0.005$ ) and more pronounced than in the UIR ( $p < 0.05$ ) and UIR + CR (no significant differences) groups (Fig. 1E and F). Thus, kidney indexes show that the UIR + KD group has greater changes than the UIR + CR group.

Histochemical analysis of fibrosis progression by Masson trichrome staining showed an increase in collagen content in the kidneys after UIR in all groups (Fig. 2A). We also examined collagen content by measuring hydroxyproline (Hyp), a result of alkaline hydrolysis of connective tissue collagen, whose content increased significantly after UIR. In the UIR and UIR + KD groups, we observed a 2-fold increase in Hyp content from 600 to 1240  $\mu\text{g/g}$  tissue ( $p < 0.005$ ), while in the UIR + CR group, there was a 3-fold increase to 1670  $\mu\text{g/g}$  tissue ( $p = 0.0001$ ) compared with the Int control (Fig. 2B). We also observed the tendency to increase the  $\alpha$ -smooth muscle actin ( $\alpha$ -SMA) level by 2.4-fold in the kidneys of the UIR + CR group (Fig. 2C). Although we found higher hydroxyproline content and  $\alpha$ -SMA levels in the UIR + CR group, the differences with UIR + KD were not statistically significant.

In addition, we investigated the influence of CR and KD on the development of renal fibrosis after UIR by examining the expression of *Col1a1*, *Col4a1*, *TGF $\beta$ 1*, *MMP2*, *Timp2* genes (Fig. 3A–E), which play a role in fibrosis development [18–20]. The expression of *Col1a1* was significantly increased in the UIR (by 10-fold,  $p < 0.005$ ) and UIR + KD (by 8-fold,  $p < 0.05$ ) groups compared to the Int group (Fig. 3A), while *TGF $\beta$ 1* expression in the kidneys of all mice increased 3–3.5-fold after UIR ( $p < 0.05$  in UIR and UIR + KD groups,  $p < 0.005$  in UIR + CR group) (Fig. 3C). *Timp2* expression was increased in the UIR (by 4.4-fold,  $p < 0.005$ ) and UIR + diets (by 4–5.7-fold) groups, with the highest levels in the UIR + CR group ( $p < 0.0005$ ) (Fig. 3E). Interestingly, the mRNA expression of *Col1a1* in the UIR + CR was similar to that in the Int group (no significant differences).

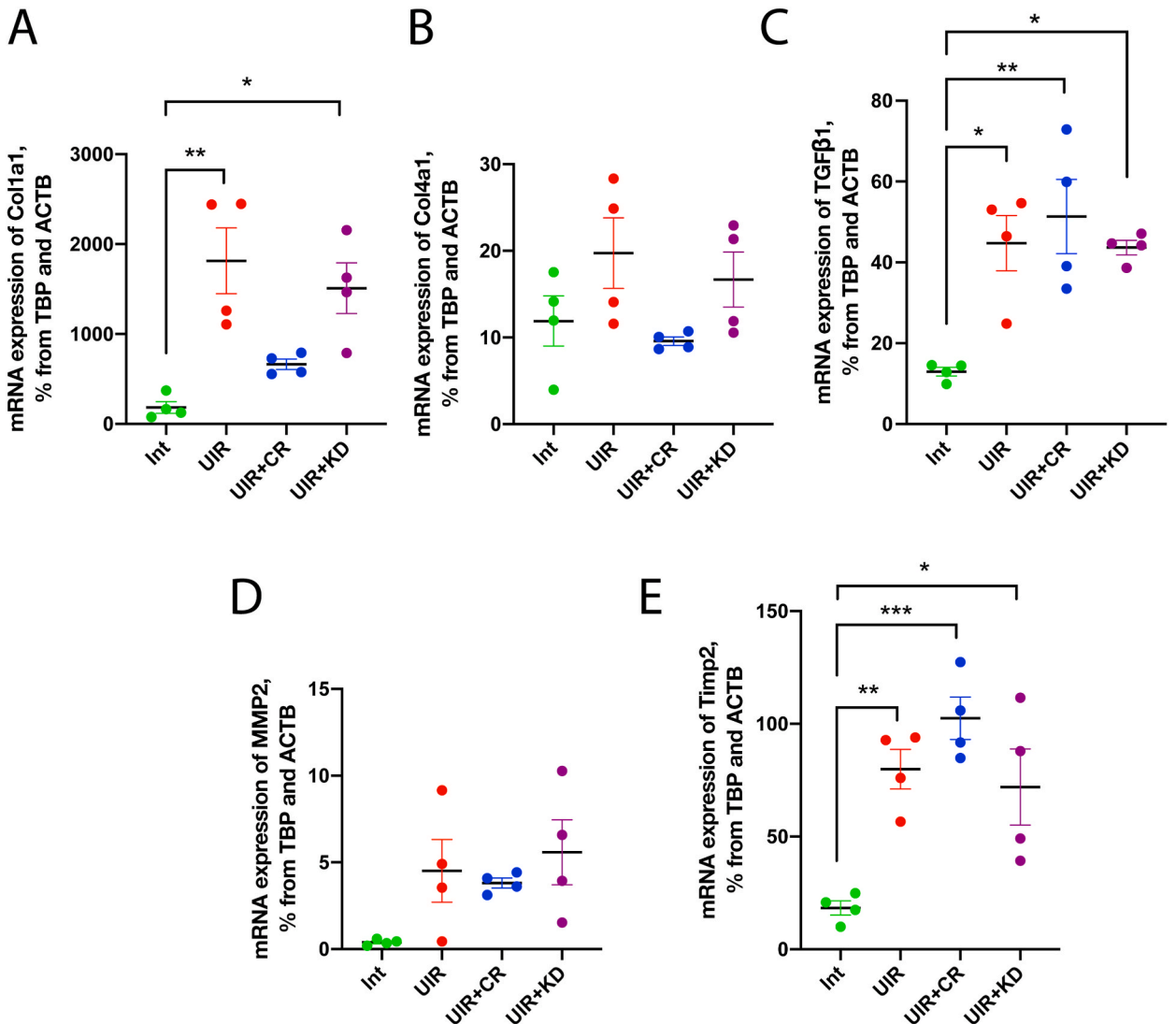
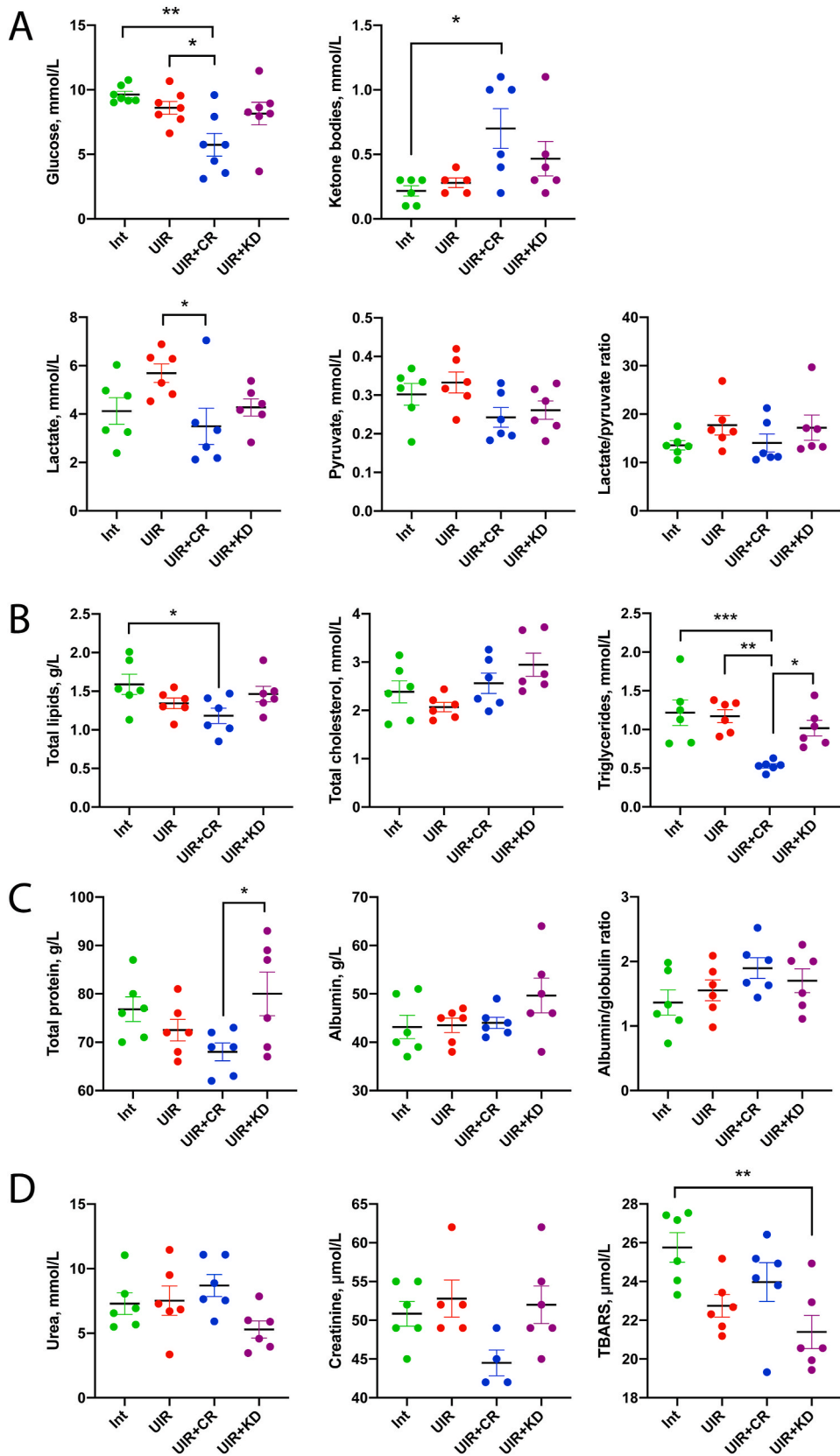


Fig. 3. mRNA expression of the genes associated with fibrosis. (A) *Col1a1*; (B) *Col4a1*; (C) *TGF $\beta$ 1*; (D) *MMP2*; (E) *Timp2*. For all groups,  $n = 4$ .



(caption on next page)

**Fig. 4.** Effect of diets on plasma levels of metabolites. (A) Major energetic metabolites. (B) Lipid metabolites. (C) Proteins. (D) Oxidative stress and AKI markers in the serum. For all groups,  $n = 6$ .

Analysis of metabolites in serum 4 weeks after UIR (Fig. 4, Table S1) showed that glucose levels were reduced 2-fold from 9.6 to 5.7 mmol/L in the UIR + CR group compared with the Int ( $p < 0.005$ ) and UIR ( $p < 0.05$ ) groups. Ketone body levels were increased 3-fold from 0.2 to 0.7 mmol/L in the UIR + CR group compared to the Int group ( $p < 0.05$ ). Lactate levels were decreased 1.5-fold from 3.5 to 5.7 mmol/L in the UIR + CR group compared with the UIR group,  $p < 0.05$  (Fig. 4A). No significant differences were observed in pyruvate levels and lactate/pyruvate ratio between all groups.

In the UIR + CR group, total lipid and triglyceride levels, but not total cholesterol, were lower than in the other groups (Fig. 4B): by 1.25-fold for total lipids ( $p < 0.05$ ) from 1.2 to 1.6 g/L and by 2.25-fold for triglyceride levels ( $p < 0.0005$ ) from 0.5 to 1.2 mmol/L. Total protein levels were significantly ( $p < 0.05$ ) 1.15-fold higher in the UIR + KD group from 72.5–80 g/L (Fig. 4C). Neither UIR nor the dietary protocols altered albumin levels and the albumin to globulin ratio. 4 weeks after UIR, markers of AKI such as urea and creatinine were not elevated in any group (Fig. 4D), indicating unaffected kidney function. KD reduced TBARS levels by 1.2-fold in the UIR + KD group compared with the Int group ( $p < 0.005$ ) from 25.8 to 21.4  $\mu\text{mol/L}$  (Fig. 4D).

We demonstrated that UIR led to a  $\sim 2$ -fold decrease in the activity of Krebs cycle enzymes in isolated mitochondria, such as  $\alpha$ -ketoglutarate dehydrogenase from 42 to 24 U/mg protein ( $p < 0.05$ ), succinate dehydrogenase from 22 to 10 U/mg protein ( $p < 0.05$ ) and malate dehydrogenase from 141 to 78 U/mg protein ( $p < 0.005$ ) ( $\alpha$ -KGDH, SDH, and MDH, correspondingly, Fig. 5A–C). Similarly,  $\alpha$ -KGDH activity was not restored in the UIR + CR group stayed 24 U/mg protein ( $p < 0.05$ ) (Fig. 5A). No significant changes were observed in citrate synthase activity and isocitrate dehydrogenase activity (CS and ICDH, correspondingly) (Fig. 5D and E)

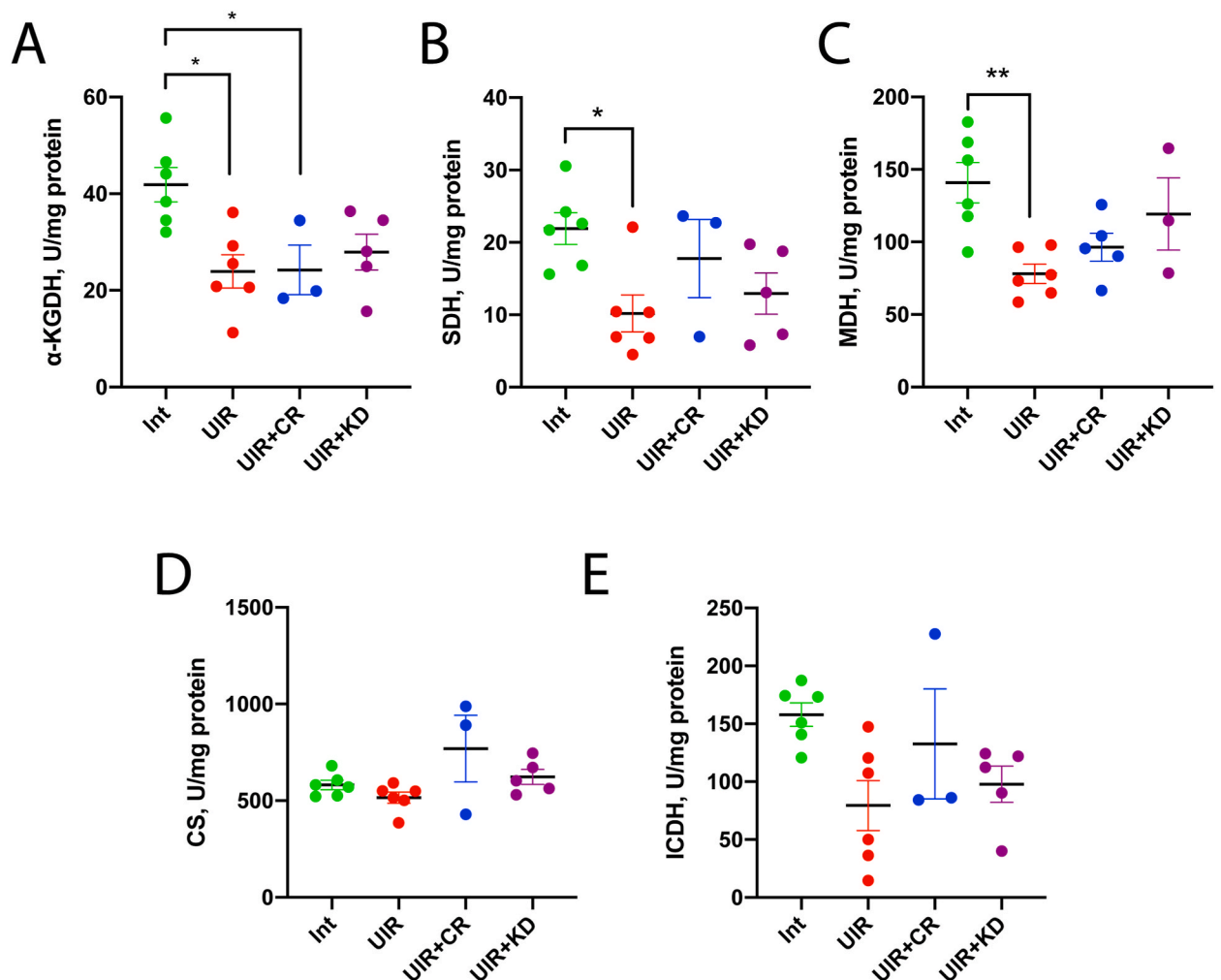


**Fig. 5.** Activity of Krebs cycle enzymes in renal mitochondria after UIR and post-treatment with different diets. (A)  $\alpha$ -ketoglutarate dehydrogenase activity. (B) Succinate dehydrogenase activity. (C) Malate dehydrogenase activity. (D) Citrate synthase activity. (E) Isocitrate dehydrogenase activity.

between all groups, although there was a trend toward a decrease in 2-fold of ICDH in the UIR group from 157 to 79 U/mg protein ( $p = 0.06$ ).

In the UIR, UIR + CR, or UIR + KD groups, the rate of glycolysis measured in the kidneys did not change 4 weeks after injury (Fig. 6A). Among glycolysis enzymes, the only significant difference was phosphofructokinase (PFK) activity, which was increased 1.5-fold after UIR from 460 to 636 U/mg protein ( $p = 0.09$ ) and decreased to normal levels in the UIR + KD group to 421 U/mg protein ( $p < 0.05$ ) (Fig. 6B). We did not observe any differences in the activities of other glycolysis enzymes (Fig. 6C–F).

Renal redox status was indirectly estimated by measuring antioxidant enzymes activity 4 weeks after UIR with different diets. However, we did not detect significant differences (see Fig. S3).

### 3. Discussion

Renal pathologies are one of the leading causes of mortality in the world and the treatment of these diseases is a huge financial burden. In this regard, the development of effective therapeutic approaches for kidney diseases, but the success in this direction has been very modest. Rapid progression of renal disease from AKI to CKD and end-stage renal disease are primarily associated with tissue remodeling and fibrosis.

The formation of renal fibrosis is a complex multicomponent process involving activation of mesangial cells and fibroblasts, tubular epithelial-to-mesenchymal transition [21], monocytes/macrophage infiltration, etc. [22]. Excessive activation of the immune response leads to glomerulosclerosis and tubulointerstitial fibrosis, which causes tubular atrophy, capillary loss, and podocyte depletion [23]. All components of this pathological process may become potential targets for the regulation of fibrosis formation. In addition, degradation of extracellular matrix components by proteolytic enzymes may also be considered as a target to reduce fibrosis, but the available data are controversial [24–27].

However, regardless of the spatial origin of renal fibrosis, it is an energy-dependent process, in which substrate and energy supply are critical for the synthesis and degradation of fibrotic elements. Modulation of energy metabolism may allow recovery of damaged tissue and attenuate the development of fibrosis. One of the most effective to intervene externally in energy metabolism is to influence diet. CR and KD are two examples of therapeutic strategies that have already demonstrated their efficacy in various disease models.

KD, a diet low in carbohydrates and high in fat, has been used to treat epilepsy since the 1920s, and there have been attempts to use

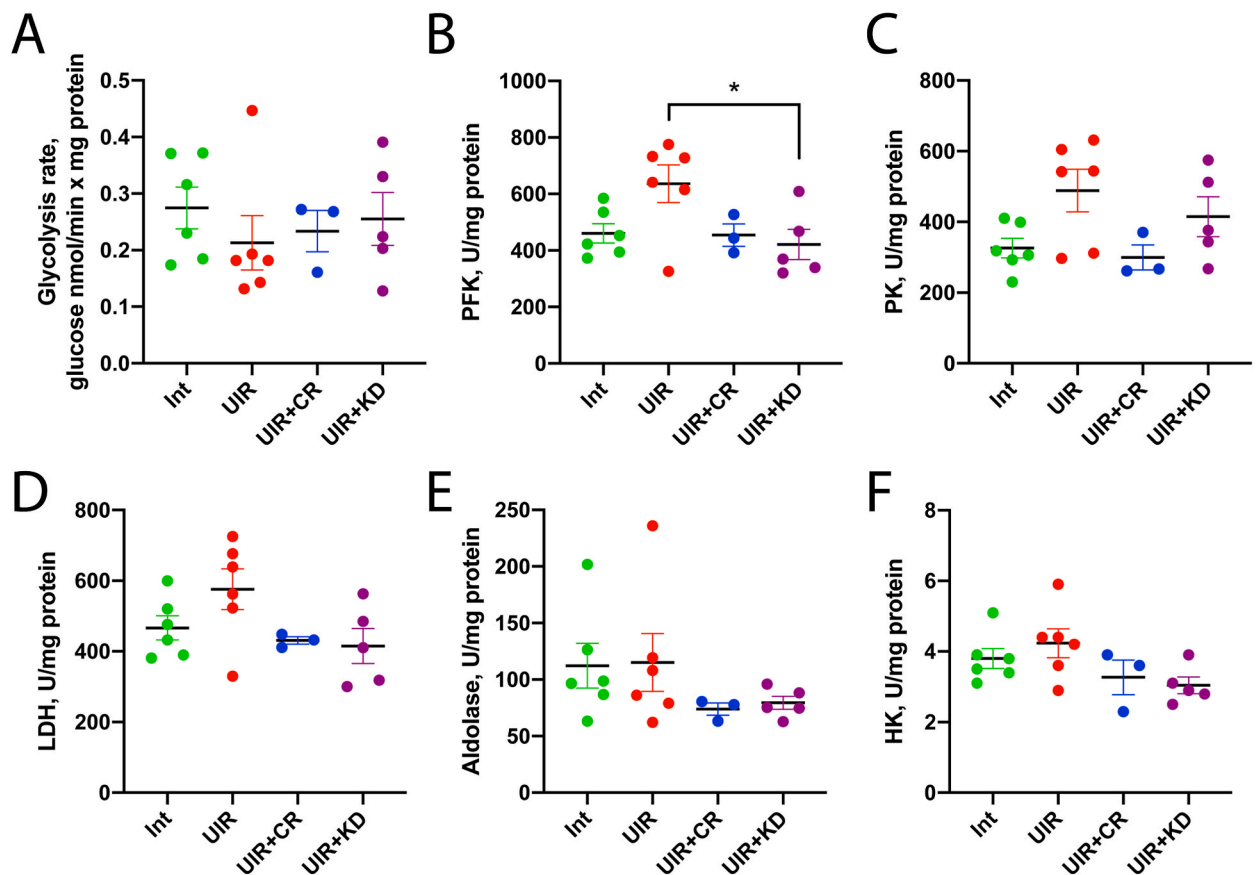


Fig. 6. Glycolysis rate and glycolysis enzymes activity in the kidneys after UIR and different diets. (A) Glycolysis rate. (B) Phosphofructokinase activity. (C) Pyruvate kinase activity. (D) Lactate dehydrogenase activity. (E) Aldolase activity. (F) Hexokinase activity.

KD against some ischemic pathologies of various organs [28]. Today, standard KD consists of a ratio of four parts fat (long-chain triglycerides) to one-part combined protein and carbohydrate, supplemented with vitamins and minerals. It is known that a 3-day KD increases tolerance to experimental kidney ischemia, reduces the number of injured tubules, and preserves renal function [16], while exogenous ketones reduce oxidative stress, inflammation, cell death, and fibrosis in the kidney [29]. Previously, limiting food intake by 35 % (35 % CR) was also found to have a protective effect in AKI [12]. In addition, fasting protects against the development of tubulointerstitial fibrosis [14]. In other studies, researchers demonstrated that fasting mediated protection against renal injury and fibrosis development after ischemic AKI [15]. In all cases, dietary interventions were performed before surgery. However, how CR and KD post-treatment may affect fibrosis development after kidney ischemia is still unknown.

In our study, we demonstrated that KD post-treatment did not affect fibrosis development 1 month after 30-min UIR, but CR post-treatment tended to stimulate fibrosis in the kidney through an additional increase in fibrosis markers such as Hyp content, mRNA expression of *Timp2*, and  $\alpha$ -SMA level (Fig. 7).

It should be noted that although  $\alpha$ -SMA is commonly cited as a marker of activated fibroblasts, there is data showing that  $\alpha$ -SMA appears to be an inconsistent marker of fibrogenesis [52]. Myofibroblasts with  $\alpha$ -SMA expression did not play a significant role in bleomycin-stimulated pulmonary fibrosis or unilateral ureteral obstruction kidney fibrosis, although they make a significant contribution to CCl<sub>4</sub>-induced liver fibrosis [30]. Also, myofibroblasts present in skeletal muscle during fibrosis do not express  $\alpha$ -SMA, and the level of  $\alpha$ -SMA expression by intramuscular fibrogenic cells did not correlate with the level of collagen gene expression or with the severity of skeletal muscle fibrosis in mdx5cv mice [31]. Thus, not all cells express  $\alpha$ -SMA that can be attributed to fibrogenic cells, and it is tissue-dependent [30,31]. In our experiment, we also demonstrated a statistically non-significant increase in  $\alpha$ -SMA levels in the IR model of kidney fibrosis.

Moreover, CR caused significant changes in circulating metabolites in the blood (Fig. 4). Specifically, (1) glucose levels were reduced in the UIR + CR group compared to the Int group as well as the UIR group; (2) ketone bodies were increased in the UIR + CR group compared with the Int group; (3) lactate levels were decreased in the UIR + CR group compared with the UIR group; (4) total lipids were lower in the UIR + CR group compared with the Int group; (5) triglyceride levels were also lower in the UIR + CR group compared with all other groups; (6) total protein levels were lower in the UIR + CR group compared with the UIR + KD group (Summarized in Fig. 8). Lower TBARS levels and higher total protein levels were observed in mice in the UIR + KD group compared with the mice in the Int group (Fig. 8).

A number of studies have demonstrated metabolic alterations associated with the development of fibrosis, most of which involve increased glycolysis and decreased fatty acid  $\beta$ -oxidation pathway (for a review, see Refs. [5,7]). The most important experiments showing metabolic reprogramming were performed in fibroblasts *in vitro*, but few experiments showed the energetic changes *in vivo* [5]. In particular, these effects were shown in induced lung fibrosis in C57BL/6J mice [32], in four models of nonalcoholic steatohepatitis in mice and rats [33], in bleomycin and TGF $\beta$ -induced lung fibrosis models [34].

In our study, we observed *in vivo* that fibrosis after UIR was accompanied by elevated serum lactate levels (Fig. 4A). It appears that fibrosis in the kidney is associated with an increase in glycolysis [5]. However, we did not observe changes in glycolysis specific enzymatic activity in the UIR group (Fig. 6). We speculate that the effects on glycolysis may be due to the blockage of pyruvate dehydrogenase, which prevents the entry of acetyl-CoA into the Krebs cycle. In kidneys, a decrease in the activity of some Krebs cycle enzymes in mitochondria ( $\alpha$ -KGDH, SDH, and MDH) by  $\sim$ 2-fold was observed after UIR (Fig. 5). On this basis, we hypothesize that pyruvate accumulates in the kidneys because it cannot be metabolized in the Krebs cycle, and is either converted to lactate (which we can see in serum) or undergoes a chain of chemical reactions for the de novo synthesis of glycine from serine [35]. TGF $\beta$ 1-induced expression of the enzymes of de novo serine and glycine synthesis has been demonstrated in fibroblasts *in vitro* [36,37]. Proline and glycine are produced directly from glutamate and account for 57 % of the amino acid content of collagen [38]. On the other hand, TGF $\beta$ 1 enhances glutamine metabolism [39]. Glutaminolysis promotes translation and stability of collagen and hydroxylation of proline [40]. The increased mRNA expression of TGF $\beta$ 1 in the UIR and UIR groups with dietary post-treatment (Fig. 3C) may indicate

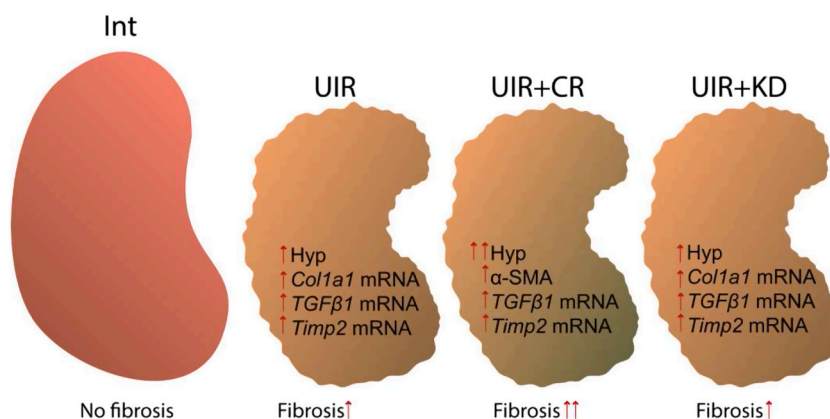


**Fig. 7.** The influence of CR and KD on fibrosis development after left kidney ischemia/reperfusion. Elevated fibrosis markers are shown as red arrows. (For interpretation of the references to color in this figure legend, the reader is referred to the Web version of this article.)

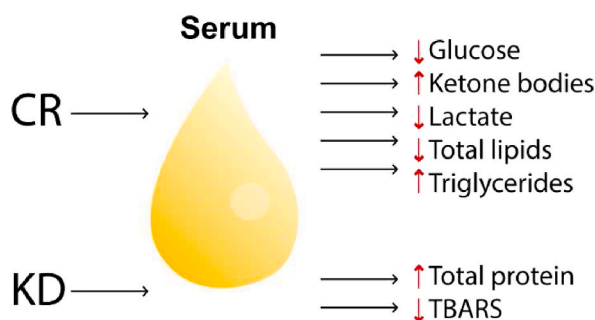


**Fig. 8.** The effect of CR and KD on serum parameters in mice 1 month after UIR. Red arrows show changes (increase/decrease). (For interpretation of the references to color in this figure legend, the reader is referred to the Web version of this article.)

activation of fibrogenic metabolic pathways in the kidneys.

Lactate is known to regulate fibrosis via lowering extracellular pH, as acidic pH induces the transition of so-called latent extracellular TGF $\beta$ 1 to the active form [41]. Moreover, lactate may serve as an additional energy source for fibroblasts [41,42]. In our study, we demonstrated a significant decrease in serum lactate levels in mice after UIR + CR (Fig. 4A). The fibrogenic process seems to be lower in this group of mice compared with UIR only or UIR with KD.

We also found that CR abolished the effect of UIR, stimulated succinate dehydrogenase, and decreased malate dehydrogenase activity but did not affect glycolysis. We showed similar results for KD, which also attenuated the effects of UIR, normalized  $\alpha$ -ketoglutarate dehydrogenase activity, and led to a decrease in phosphofructokinase activity (Figs. 5 and 6, Table 1).

As we see, energy metabolism is suppressed in the UIR group and we hypothesize that renal function may be reduced after UIR, whereas the contralateral kidney compensates. For this reason, we do not see an increase in blood urea and creatinine levels in mice with UIR (Fig. 4D). Indeed, we observed not only a decrease in the size of the UIR kidney (Fig. 1D) but also an increase in the contralateral kidney size (Fig. 1E), which looks like compensatory hypertrophy. To confirm the decreasing renal function 1 month after ischemia/reperfusion injury, we measured blood urea and creatinine levels in animals subjected to UIR with contralateral nephrectomy (see Fig. S4).

The main focus of metabolic changes during kidney fibrosis is glycolysis. Inhibitors of glycolysis (dichloroacetate, shikonin, and 2-deoxyglucose) have been shown to suppress an increase in the synthesis of ECM proteins [34,43] and attenuate renal fibrosis in a UUO mouse model [7,44]. On the contrary, in a diabetic kidney model, an increase in glycolysis resulted in decreased expression of fibrotic proteins [45]. Furthermore, using transgenic mice with a mutation in the 6-phosphofructo-2-kinase/fructose-2,6-biphosphatase, it was shown that reduced glycolysis was associated with increased renal fibrosis in the UUO mouse model and, to a lesser extent, in the folic acid nephropathy model [46]. Thus, the role of energy metabolism in renal fibrosis is complex, and the effect may depend on cell types and stage of fibrosis development [47]. In our study, we did not observe any effects on renal fibrosis by CR and KD associated with changes in energy metabolism.

We should note that in our experiment we did not observe elevated urea and creatinine blood levels in the UIR group and UIR with diets. We assume this could be due to the omission of contralateral nephrectomy in our experiment. Contralateral kidney seems to provide functional compensation for waste metabolites excretion. In this situation, injured kidney could faster normalized its metabolism (glycolysis, Krebs's cycle, redox status). It should be noted that kidney fibrosis is a dynamic process and that longer-term therapeutic manipulation including diets can have a greater effect on fibrosis resolution. It has already been described previously that the most pronounced effects of diets were observed with prolonged exposure, especially with long-term caloric restriction. With this in mind, we cannot rule out beneficial effects of the diets studied when animals were treated for longer than 1 month. However, further studies are needed to test these assumptions.

Ultimately, kidney ischemia/reperfusion leads to the development of renal fibrosis associated with metabolic suppression of the tricarboxylic acid cycle but not glycolysis. CR and KD administered for 1 month after kidney ischemia/reperfusion affected metabolism but had no significant effect on reducing renal fibrosis. Further studies are needed to explore the molecular mechanisms of the induced metabolic abnormalities during the progression of renal fibrosis and to develop successful targeted therapies.

**Table 1**  
Summarized metabolic changes during fibrosis development after UIR and dietary intervention.

Intervention	Krebs cycle enzymes	Glycolysis
UIR	↓ $\alpha$ -KGDH ↓ SDH ↓ MDH	No changes
UIR + CR	↓ $\alpha$ -KGDH	No changes
UIR + KD	No changes	↓ PPK

Arrows demonstrate the decrease of enzyme activity.

### 3.1. Limitations of the study

In our study, we for the first time investigated how dietary approaches such as CR and KD can affect fibrosis development after ischemia/reperfusion in mice. Although we observed some changes in renal tissue energy metabolism in the mice after the diets, human metabolism may differ. Therefore, it may be difficult to extrapolate our data to human renal pathologies. But we can investigate such pathologies with specific treatment only in animal ischemia/reperfusion models. Although we observed that the CR and KD post-treatment did not reduce fibrosis development, we do not exclude that the pre-treatment may have a beneficial effect on AKI. In our experiments, we used the ischemia/reperfusion model without contralateral nephrectomy and observed many metabolic parameters unchanged. It is probable that a model with the nephrectomy might induce greater changes.

## 4. Star methods

### 4.1. Animals

Healthy male BALB/c mice 12 weeks of age (30–39 g) were housed under controlled conditions with a 12-h light/dark cycle at  $22 \pm 2^\circ\text{C}$  and used for commonly performed ischemia/reperfusion injury model of renal pathology [48,49]. Mice were used according to animal protocols evaluated and approved by the animal ethics committee of the A.N. Belozersky Institute of Physico-Chemical Biology: Protocol 2/20 from February 12, 2020. All procedures were in accordance with Federation of Laboratory Animal Science Associations (FELASA) guidelines.

### 4.2. Experimental design

AKI was induced by UIR without contralateral nephrectomy as previously described [50]. Briefly, mice were anesthetized with isoflurane. Animals were placed supine on a heating pad and the left renal vascular bundle was occluded with a microvascular clip for 30 min. After ischemia, circulation was restored by removing the clip. During the surgical procedure, the body temperature of the rats was maintained at  $37 \pm 0.5^\circ\text{C}$  by heating pad. Mice were divided into groups: Intact control (Int) with normal rodent chow diet *ad libitum*; UIR with normal diet *ad libitum* before and after surgery; UIR followed by dietary restriction by 35 % [13] (UIR + CR); UIR followed by diet with ketogenic diet [16] (C1084, Altromin) (UIR + KD). Urine samples were collected before surgery and 24 h after.

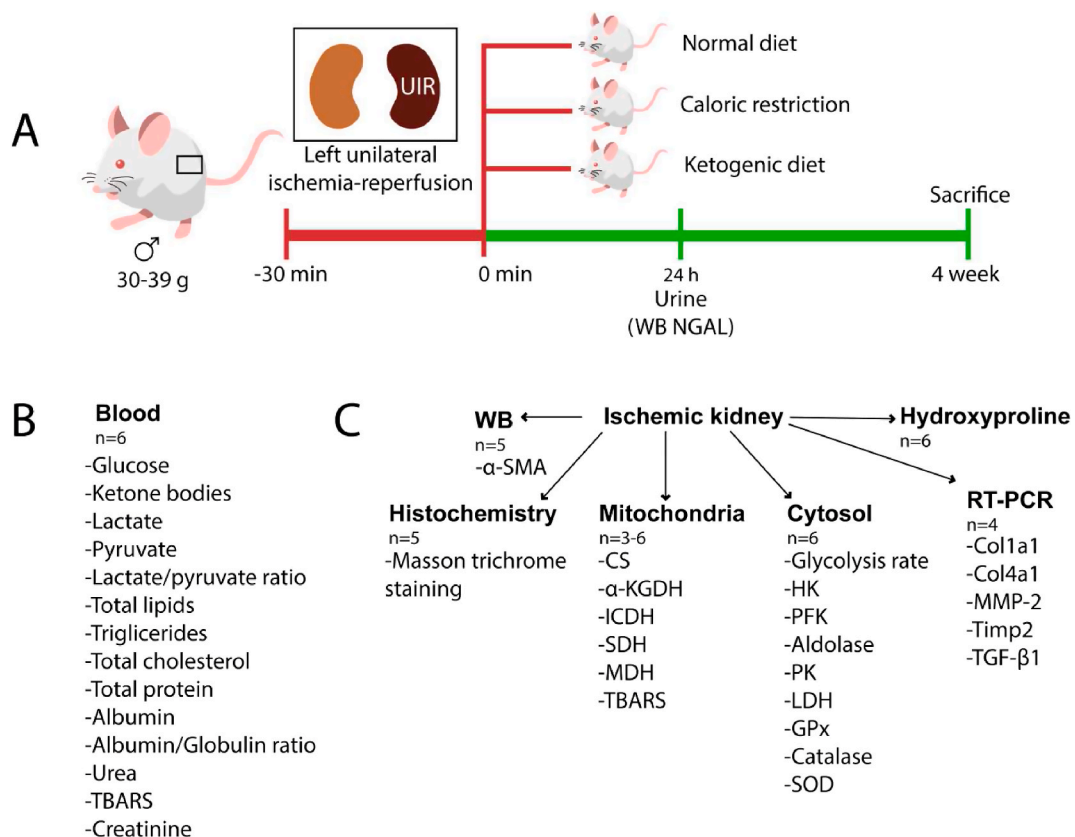


**Fig. 9.** Experimental design. (A) The timing schedule. (B) Analyzed parameters in blood. (C) Analyzed parameters in ischemic kidney.

Mice were sacrificed after 4 weeks. The entire experimental design is shown in Fig. 9A. Kidneys were photographed and kidney weight was measured. For 5 animals per group, the ischemic kidneys were removed, decapsulated, divided, and half was placed in 10 % buffered formalin while another half was homogenized in RIPA buffer for further Western blotting. The total protein content in the samples was measured using a commercial bicinchoninic acid-based kit (Sigma, Burlington, USA). In 6 animals per group, the blood and left kidney were collected for hydroxyproline measurement and mitochondria/cytosol isolation with further biochemical analysis (Fig. 9B and C). For 4 animals per group kidney tissue was collected for RT-PCR analysis (Fig. 9C). The kidney index was estimated as the ratio of kidney weight to body weight expressed as a percentage. The kidney index was estimated using the following formula:

$$\text{Kidney index} = \frac{\text{Kidney weight}}{\text{Body weight}} * 100$$

#### 4.3. Dietary protocols

Food intake of each mouse was measured for one week before surgical procedures. CR was performed for 4 weeks after the surgery by limiting the amount of food by 35 % of the daily intake. Food was administered once daily at 12:00 noon. In the KD group, mice were fed ketogenic chow (Altromin C 1084, Germany) *ad libitum* after surgery. Free access to water was provided for all groups. Weekly, each mouse was weighed to monitor the changes in body mass.

#### 4.4. Western blotting

Western blotting was performed by the conventional method under denaturing conditions. Samples were loaded into the gel (10 µg total protein per well for kidney and 15 µL for urine) and transferred to a PVDF membrane (Amersham Pharmacia Biotech, Buckinghamshire, UK) after electrophoretic separation. Membranes were blocked in 5 % milk in PBS containing 0.05 % Tween-20 for 45 min at room temperature and incubated with primary antibodies, followed by three washes. Primary antibodies were diluted in 0.1 % BSA solution in PBS + Tween-20 and used at the following dilutions: anti-NGAL rabbit 1:1000 (Abcam, Cambridge, UK), anti-α-SMA rabbit 1:1000 (Abcam, UK), anti-β-actin mouse 1:2000 (Sigma, USA). Membranes were incubated overnight with the primary antibodies at 4 °C, washed, and incubated with secondary goat anti-rabbit or anti-mouse IgG antibodies conjugated to horseradish peroxidase (IMTEK, Russia; dilution 1:10000) for 60 min at 37 °C. After washing, membranes were incubated for 5 min with the Advansta ECL Bright chemiluminescence kit (Advansta, San Jose, CA, USA) and scanned with the ChemiDoc MP Imaging System (BioRad, Hercules, CA, USA). Band luminescence intensity was quantified using ImageLab software (BioRad, Hercules, CA, USA).

#### 4.5. Histological analysis

Fixed tissues were cut into 4 µm sections and stained using the Masson trichrome protocol. Stained kidney sections were viewed using an Axio Scope A1 microscope (Carl Zeiss, Germany) with MRc.5 camera (Carl Zeiss, Germany). On each slide, three images of cortex and medulla were randomly selected for analysis. Sections were examined in a blinded fashion for fibrosis.

#### 4.6. Hydroxyproline measurement

The method is based on the alkaline hydrolysis of tissue and subsequent quantification of free hydroxyproline (Hyp) in the hydrolyzates [51]. Kidney tissues (20 mg) were placed in 0.5 ml of 7 M KOH and hydrolyzed at 120 °C for 40 min. The hydrolyzate was neutralized with 3.5 M sulfuric acid and mixed with a buffered chloramine-T reagent. After 20 min at room temperature Ehrlich's reagent (Sigma-Aldrich, USA) was added for 20 min at 65°C. The optical density was measured at 550 nm on a PE-5400UV spectrophotometer ("Ekrokhim", LLC, St. Petersburg, Russia). The level of Hyp in renal tissue was estimated using a calibration curve.

#### 4.7. RT-PCR

Kidney tissue samples were placed in Intact RNA solution (Evrogen, Russia) for preserving RNA integrity and stored at –80 °C. RNA Solo kit (Evrogen, Russia) was used for nucleic acid isolation and treatment with duplex-specific nuclease. Following RNA extraction, the concentration and purity were determined by a Nanodrop spectrophotometer ND-1000 (Thermo Fisher Scientific, USA). Reverse

**Table 2**  
Primer sequences used for estimation of gene expression.

Gene name	The sequence of forward primer 5'- to 3'	The sequence of reverse primer 5'- to 3'
<i>ACTB</i>	GTACCACCATGTACCCAGGC	AACGCAGCTCAGTAACAGTCC
<i>TBP</i>	ACCGTGAATCTTGGCTGTAAC	GCAGCAAATCGCTTGGGATTA
<i>TGF1β</i>	TGATACGCCCTGAGTGGCTGTCT	CACAAGAGCAGTGAGCGTGAA
<i>MMP2</i>	CAAGTTCCCCGGCGATGTC	TTCTGGTCAAGGTCACCTGTC
<i>TIMP2</i>	TCAGAGCCAAAGCAGTGAGC	GCCGTGTAGATAAACTCGATGTC
<i>Col4a1</i>	ATGGCTTGCCTGGAGAGATAGG	TGGTTGCCCTTTGAGTCTCGGA
<i>Col1a1</i>	CGATGGATTCCCGTTTCGAGT	CGATCTCGTTGGATCCCTGG

transcription was performed using the MMLV RT kit (Evrogen, Russia). The RT-PCR was performed on Bio-Rad Real-Time PCR System (Bio-Rad, California, Hercules, CA, USA) by using SYBR Green as a double-strand DNA-specific binding dye. Amplification was carried out using 5X qPCRmix-HS mastermix (Evrogen, Russia). Amplification modes: 95°C 5 min; 95°C 10 s; 58°C 17 s; 72°C 20 s; 40 repetitions of steps 95°C 10 s, 58°C 17 s, 72°C 20 s; melting curve from 72 to 95°C, increment 0.5°C 5 s. The selection of primers (Table 2) was performed using the Beacon Designer 7 program (Premier Biosoft Int., USA), as well as using the NCBI and BLAT search databases. The primers were synthesized by DNA-synthesis (Moscow, Russia). Their efficiencies were calculated by generating a standard curve for each target gene using a five-fold serial dilution of the cDNA pool and were in the range of 1.8–2.0. mRNA expression levels were calculated as  $E^{-Ct}$ , where  $E$  is the primer efficiency and  $Ct$  are the cycle number on which product fluorescence rose above the threshold level. These values were normalized to the geometric mean of the threshold cycles of two housekeeping genes ( $\beta$ -actin (ACTB) and TATA-box-binding protein (TBP)), to level individual differences between animals [52].

#### 4.8. Biochemical analysis of the blood

Blood plasma was obtained by centrifugation of heparinized blood at 3000 rpm for 10 min and stored at  $-80^{\circ}\text{C}$ . The total protein content was determined by the BCA method using a commercial kit (Sigma, USA). Serum albumin, creatinine, urea, total plasma lipids, triglycerides and total cholesterol were measured. The content of lipid peroxidation products (TBA-reactive substances, TBARS) in plasma was determined by the reaction with 2-thiobarbituric acid (TBA) [53]. The measurements were carried out on a FluoroMax-3 spectrofluorometer ("HORIBA Jobin Yvon", UK) at an extinction wavelength of 515 nm and an emission wavelength of 553 nm. The concentration of ketone bodies in plasma was determined using a portable ketometer (CareSens Dual, i-SENS Inc, South Korea).

For determination of glucose, pyruvate, and lactate blood was mixed with 6 % perchloric acid in a ratio of 1:1 (v/v), placed on ice for 15 min, and centrifuged at 12,000 rpm for 10 min at  $4^{\circ}\text{C}$ . The supernatant was adjusted to pH 7 with saturated potassium carbonate solution, placed on ice for 15 min, and centrifuged at 12,000 rpm for 3 min at  $4^{\circ}\text{C}$ . Glucose and lactate concentrations were determined by enzymatic methods based on the Trinder reaction using commercial kits (Olveks Diagnosticum, Russia). The pyruvate concentration was determined by the enzymatic method with lactate dehydrogenase [54]. The measurements were carried out on a PE-5400UV spectrophotometer ("Ekroskhim") at a wavelength of 340 nm.

#### 4.9. Isolation of kidney mitochondria

Left kidneys were removed, weighed, and homogenized in a cold isolation medium containing 250 mM sucrose, 10 mM Tris HCl and 1 mM EDTA, with a pH of 7.4 at a ratio of 1:10 (w/v). Mitochondria were isolated using differential centrifugation [55]. Mitochondrial pellets were washed twice with the isolation medium and resuspended in a hypotonic buffer (10 mM Tris HCl, 0.5 mM EDTA) to final protein concentration of 5–10 mg/mL. Concentrations of total protein were determined using the Peterson method [56]. Supernatant after mitochondria sedimentation was used for cytosol investigation.

#### 4.10. Determination of Krebs cycle enzymes activity

To determine the activity of Krebs cycle enzymes, mitochondria were subjected to three freeze–thaw cycles. The activity of citrate synthase (CS, EC 2.3.3.16) was determined by a kinetic method based on the non-enzymatic reaction of coenzyme A (CoA-SH) with Ellman's reagent [57]. The activity of NADP-dependent isocitrate dehydrogenase (ICDH, EC 1.1.1.42) was determined by a kinetic method based on the absorption of NADPH [58]. The activity of  $\alpha$ -ketoglutarate dehydrogenase ( $\alpha$ -KGDH, EC 1.2.4.2) and succinate dehydrogenase (SDH, EC 1.3.5.1) was assessed spectrophotometrically using potassium ferricyanide as an electron acceptor [59,60].

The activity of malate dehydrogenase (MDH, EC 1.1.1.37) was determined by the kinetic method by reducing the absorption of NADH [61].

The absorbance was measured by Zenith 1100 plate reader in the "Kinetics" mode at a temperature of  $37^{\circ}\text{C}$  in a 96-well plate. As 1 unit (U) of activity of ICDH and MDH, 1 nmol of NAD(P)H formed (or consumed) in 1 min at temperature  $37^{\circ}\text{C}$  was taken. As 1 unit (U) of  $\alpha$ -KGDH and SDH activity 1 nmol of potassium ferricyanide reduced in 1 min at a temperature of  $37^{\circ}\text{C}$  was taken.

#### 4.11. Determination of the glycolysis rate and the activity of glycolytic enzymes

The rate of glycolysis was estimated by the Allen method [61] with modifications. The method is based on the change in glucose concentration during incubation of the tissue extract of the kidneys (cytosolic fraction) in the presence (control tubes) and in the absence (test tubes) of the hexokinase inhibitor - 2-deoxy-D-glucose [62]. Concentration of glucose was determined by commercial reagent kit (Olveks Diagnosticum, Russia). Glycolysis rate was expressed in nmol of D-glucose utilized in 1 min by 1 mg of cytosolic protein (nmol/min  $\times$  mg of protein).

The activities of hexokinase (HK, EC 2.7.1.1) [63], phosphofructokinase (PFK, EC 2.7.1.11) [64], pyruvate kinase (PK, EC 2.7.1.40) [65] and lactate dehydrogenase (LDH, EC 1.1.1.27) [66] were determined by kinetic methods based on the absorption of NAD(P)H at 340 nm. The absorbance was measured in the "Kinetics" mode at a temperature of  $37^{\circ}\text{C}$  in a 96-well plate on a Zenit 1100 multi-detector. As 1 unit (U) of enzyme activity, 1 nmol of NAD(P)H formed (or consumed) in 1 min at a temperature of  $37^{\circ}\text{C}$  was taken.

Aldolase activity was determined by a colorimetric method based on the reaction of 2,4-dinitrophenylhydrazine with phosphotrioses in an alkaline medium [67]. As 1 unit of aldolase activity (U), 1 nmol of phosphotriose, formed from fructose-1,6-bisphosphate in 1 min at a temperature of  $37^{\circ}\text{C}$  was taken.

#### 4.12. Statistical analysis

Statistical analysis was performed with the GraphPad Prism 7 (GraphPad Software Inc., USA). The data was analyzed by parametric one-way ANOVA with Sidak's multiple comparison test or nonparametric Kruskal-Wallis test followed by Dunn's multiple comparison test based on their distribution normality (Shapiro-Wilk normality test). The results are presented as mean  $\pm$  SEM with a  $*p < 0.05$ ,  $**p < 0,005$ ,  $***p < 0,0005$ ,  $****p = 0,0001$  considered as statistically significant. T-test and Mann-Whitney U test were used for pairwise comparison of body weight between UIR and UIR + CR group.

#### Funding

This work was supported by the Russian Science Foundation (grant #21-75-30009).

#### CRedit authorship contribution statement

**E.I. Yakupova:** Investigation, Writing – original draft. **D.S. Semenovich:** Investigation, Methodology. **P.A. Abramicheva:** Investigation. **L.D. Zorova:** Investigation. **I.B. Pevzner:** Investigation. **N.V. Andrianova:** Investigation, Validation. **V.A. Popkov:** Investigation. **V.N. Manskikh:** Investigation. **A.D. Bocharnikov:** Investigation. **Y.A. Voronina:** Investigation. **D.B. Zorov:** Validation, Writing - review & editing. **E.Y. Plotnikov:** Conceptualization, Funding acquisition, Project administration, Supervision, Writing – review & editing.

#### Declaration of competing interest

The authors declare the following financial interests/personal relationships which may be considered as potential competing interests:

Egor Plotnikov reports financial support was provided by Russian Science Foundation.

#### Appendix A. Supplementary data

Supplementary data to this article can be found online at <https://doi.org/10.1016/j.heliyon.2023.e21003>.

#### References

- [1] J.S. Duffield, Cellular and molecular mechanisms in kidney fibrosis, *J. Clin. Invest.* 124 (2014) 2299–2306.
- [2] B.D. Humphreys, Mechanisms of renal fibrosis, *Annu. Rev. Physiol.* 80 (2018) 309–326.
- [3] T.J. Keane, C.-M. Horejs, M.M. Stevens, Scarring vs. functional healing: matrix-based strategies to regulate tissue repair, *Adv. Drug Deliv. Rev.* 129 (2018) 407–419.
- [4] GBD Chronic Kidney Disease Collaboration, Global, regional, and national burden of chronic kidney disease, 1990–2017: a systematic analysis for the Global Burden of Disease Study 2017, *Lancet* 395 (2020) 709–733.
- [5] E.I. Yakupova, D.B. Zorov, E.Y. Plotnikov, Bioenergetics of the fibrosis, *Biochemistry (Moscow)* 86 (2021) 1599–1606, <https://doi.org/10.1134/s0006297921120099>.
- [6] X. Wei, Y. Hou, M. Long, L. Jiang, Y. Du, Advances in energy metabolism in renal fibrosis, *Life Sci.* 312 (2023), 121033.
- [7] Q. Wei, J. Su, G. Dong, M. Zhang, Y. Huo, Z. Dong, Glycolysis inhibitors suppress renal interstitial fibrosis via divergent effects on fibroblasts and tubular cells, *Am. J. Physiol. Renal Physiol.* 316 (2019) F1162–F1172.
- [8] L.T. Robertson, J.R. Mitchell, Benefits of short-term dietary restriction in mammals, *Exp. Gerontol.* 48 (2013) 1043–1048.
- [9] S.R. Spindler, Caloric restriction: from soup to nuts, *Ageing Res. Rev.* 9 (2010) 324–353, <https://doi.org/10.1016/j.arr.2009.10.003>.
- [10] G. López-Lluch, P. Navas, Calorie restriction as an intervention in ageing, *J. Physiol.* 594 (2016) 2043–2060.
- [11] O.A. González, C. Tobia, J.L. Ebersole, M.J. Novak, Caloric restriction and chronic inflammatory diseases, *Oral Dis.* 18 (2012) 16–31, <https://doi.org/10.1111/j.1601-0825.2011.01830.x>.
- [12] N.V. Andrianova, L.D. Zorova, I.B. Pevzner, V.A. Popkov, V.P. Chernikov, D.N. Silachev, E.Y. Plotnikov, D.B. Zorov, Resemblance and differences in dietary restriction nephroprotective mechanisms in young and old rats, *Ageing* 12 (2020) 18693–18715.
- [13] N.V. Andrianova, M.I. Buyan, A.K. Bolikhova, D.B. Zorov, E.Y. Plotnikov, Dietary restriction for kidney protection: Decline in nephroprotective mechanisms during aging, *Front. Physiol.* 12 (2021), 699490.
- [14] P. Rojas-Morales, J.C. León-Contreras, O.E. Aparicio-Trejo, J.G. Reyes-Ocampo, O.N. Medina-Campos, A.S. Jiménez-Osorio, S. González-Reyes, B. Marquina-Castillo, R. Hernández-Pando, D. Barrera-Oviedo, L.G. Sánchez-Lozada, J. Pedraza-Chaverri, E. Tapia, Fasting reduces oxidative stress, mitochondrial dysfunction and fibrosis induced by renal ischemia-reperfusion injury, *Free Radic. Biol. Med.* 135 (2019) 60–67.
- [15] P. Rojas-Morales, E. Tapia, J.C. León-Contreras, S. González-Reyes, A.S. Jiménez-Osorio, J. Trujillo, N. Pavón, J. Granados-Pineda, R. Hernández-Pando, L. G. Sánchez-Lozada, H. Osorio-Alonso, J. Pedraza-Chaverri, Mechanisms of fasting-mediated protection against renal injury and fibrosis development after ischemic acute kidney injury, *Biomolecules* 9 (2019), <https://doi.org/10.3390/biom9090404>.
- [16] P. Rojas-Morales, J.C. León-Contreras, M. Sánchez-Tapia, A. Silva-Palacios, A. Cano-Martínez, S. González-Reyes, A.S. Jiménez-Osorio, R. Hernández-Pando, H. Osorio-Alonso, L.G. Sánchez-Lozada, A.R. Tovar, J. Pedraza-Chaverri, E. Tapia, A ketogenic diet attenuates acute and chronic ischemic kidney injury and reduces markers of oxidative stress and inflammation, *Life Sci.* 289 (2022), 120227.
- [17] Y. You, Y. Guo, P. Jia, B. Zhuang, Y. Cheng, H. Deng, X. Wang, C. Zhang, S. Luo, B. Huang, Ketogenic diet aggravates cardiac remodeling in adult spontaneously hypertensive rats, *Nutr. Metab.* 17 (2020) 91.
- [18] Z. Cheng, X. Zhang, Y. Zhang, L. Li, P. Chen, Role of MMP-2 and CD147 in kidney fibrosis, *Open Life Sci.* 17 (2022) 1182–1190.
- [19] R.D. Bülow, P. Boor, Extracellular matrix in kidney fibrosis: more than Just a Scaffold, *J. Histochem. Cytochem.* 67 (2019) 643–661.
- [20] Q. Yuan, B. Tang, C. Zhang, Signaling pathways of chronic kidney diseases, implications for therapeutics, *Signal Transduct Target Ther* 7 (2022) 182.

- [21] G. Campanholle, G. Ligresti, S.A. Gharib, J.S. Duffield, Cellular mechanisms of tissue fibrosis. 3. Novel mechanisms of kidney fibrosis, *Am. J. Physiol. Cell Physiol.* 304 (2013) C591–C603.
- [22] Y. Liu, Renal fibrosis: new insights into the pathogenesis and therapeutics, *Kidney Int.* 69 (2006) 213–217.
- [23] W.G. Couser, Basic and translational concepts of immune-mediated glomerular diseases, *J. Am. Soc. Nephrol.* 23 (2012) 381–399.
- [24] J. Yang, R.W. Shultz, W.M. Mars, R.E. Wegner, Y. Li, C. Dai, K. Nejak, Y. Liu, Disruption of tissue-type plasminogen activator gene in mice reduces renal interstitial fibrosis in obstructive nephropathy, *J. Clin. Invest.* 110 (2002) 1525–1538.
- [25] K.L. Edgton, R.M. Gow, D.J. Kelly, P. Carmeliet, A.R. Kitching, Plasmin is not protective in experimental renal interstitial fibrosis, *Kidney Int.* 66 (2004) 68–76.
- [26] X. Du, A. Shimizu, Y. Masuda, N. Kuwahara, T. Arai, M. Kataoka, M. Uchiyama, T. Kaneko, T. Akimoto, Y. Iino, Y. Fukuda, Involvement of matrix metalloproteinase-2 in the development of renal interstitial fibrosis in mouse obstructive nephropathy, *Lab. Invest.* 92 (2012) 1149–1160.
- [27] I.B. Pevzner, L.D. Zorova, F.A. Galkin, E.Y. Plotnikov, D.B. Zorov, Mitochondria-associated matrix Metalloproteinases 2 and 9 in acute renal pathologies, *Bull. Exp. Biol. Med.* 166 (2019) 334–338.
- [28] C.I. Makievskaia, V.A. Popkov, N.V. Andrianova, X. Liao, D.B. Zorov, E.Y. Plotnikov, Ketogenic diet and ketone bodies against ischemic injury: targets, mechanisms, and therapeutic potential, *Int. J. Mol. Sci.* 24 (2023), <https://doi.org/10.3390/ijms24032576>.
- [29] P. Rojas-Morales, J. Pedraza-Chaverri, E. Tapia, Ketone bodies for kidney injury and disease, *Adv. Redox Res.* 2 (2021), 100009.
- [30] K.-H. Sun, Y. Chang, N.I. Reed, D. Sheppard,  $\alpha$ -Smooth muscle actin is an inconsistent marker of fibroblasts responsible for force-dependent TGF $\beta$  activation or collagen production across multiple models of organ fibrosis, *Am. J. Physiol. Lung Cell Mol. Physiol.* 310 (2016) L824–L836.
- [31] W. Zhao, X. Wang, K.-H. Sun, L. Zhou,  $\alpha$ -smooth muscle actin is not a marker of fibrogenic cell activity in skeletal muscle fibrosis, *PLoS One* 13 (2018), e0191031.
- [32] R.B. Hamanaka, R. Nigdelioglu, A.Y. Meliton, Y. Tian, L.J. Witt, E. O'Leary, K.A. Sun, P.S. Woods, D. Wu, B. Ansbros, S. Ard, J.M. Rohde, N.O. Dulin, R.D. Guzy, G.M. Mutlu, Inhibition of phosphoglycerate dehydrogenase attenuates bleomycin-induced pulmonary fibrosis, *Am. J. Respir. Cell Mol. Biol.* 58 (2018) 585–593.
- [33] J. Bates, A. Vijayakumar, S. Ghoshal, B. Marchand, S. Yi, D. Kornyevev, A. Zagorska, D. Hollenback, K. Walker, K. Liu, S. Pendem, D. Newstrom, R. Brockett, I. Mikaelian, S. Kusam, R. Ramirez, D. Lopez, L. Li, B.C. Fuchs, D.G. Breckenridge, Acetyl-CoA carboxylase inhibition disrupts metabolic reprogramming during hepatic stellate cell activation, *J. Hepatol.* 73 (2020) 896–905.
- [34] N. Xie, Z. Tan, S. Banerjee, H. Cui, J. Ge, R.-M. Liu, K. Bernard, V.J. Thannickal, G. Liu, Glycolytic reprogramming in myofibroblast differentiation and lung fibrosis, *Am. J. Respir. Crit. Care Med.* 192 (2015) 1462–1474.
- [35] W. Wang, Z. Wu, Z. Dai, Y. Yang, J. Wang, G. Wu, Glycine metabolism in animals and humans: implications for nutrition and health, *Amino Acids* 45 (2013) 463–477.
- [36] R. Nigdelioglu, R.B. Hamanaka, A.Y. Meliton, E. O'Leary, L.J. Witt, T. Cho, K. Sun, C. Bonham, D. Wu, P.S. Woods, A.N. Husain, D. Wolfgeher, N.O. Dulin, N. S. Chandel, G.M. Mutlu, Transforming growth factor (TGF)- $\beta$  promotes de Novo serine synthesis for collagen production, *J. Biol. Chem.* 291 (2016) 27239–27251.
- [37] B. Selvarajah, I. Azuelos, M. Platé, D. Guillotin, E.J. Forty, G. Contento, H.V. Woodcock, M. Redding, A. Taylor, G. Brunori, P.F. Durrenberger, R. Ronzoni, A. D. Blanchard, P.F. Mercer, D. Anastasiou, R.C. Chambers, mTORC1 amplifies the ATF4-dependent de novo serine-glycine pathway to supply glycine during TGF- $\beta$ -induced collagen biosynthesis, *Sci. Signal.* 12 (2019), <https://doi.org/10.1126/scisignal.aav3048>.
- [38] P. Li, G. Wu, Roles of dietary glycine, proline, and hydroxyproline in collagen synthesis and animal growth, *Amino Acids* 50 (2018) 29–38, <https://doi.org/10.1007/s00726-017-2490-6>.
- [39] T.D. Hewitson, E.R. Smith, A metabolic reprogramming of glycolysis and glutamine metabolism is a requisite for renal fibrogenesis—why and how? *Front. Physiol.* 12 (2021) <https://doi.org/10.3389/fphys.2021.645857>.
- [40] J. Ge, H. Cui, N. Xie, S. Banerjee, S. Guo, S. Dubey, S. Barnes, G. Liu, Glutaminolysis promotes collagen translation and stability via  $\alpha$ -Ketoglutarate-mediated mTOR activation and proline hydroxylation, *Am. J. Respir. Cell Mol. Biol.* 58 (2018) 378–390, <https://doi.org/10.1165/rcmb.2017-0238oc>.
- [41] R.M. Kottmann, A.A. Kulkarni, K.A. Smolnycki, E. Lyda, T. Dahanayake, R. Salibi, S. Honnons, C. Jones, N.G. Isern, J.Z. Hu, S.D. Nathan, G. Grant, R.P. Phipps, P.J. Sime, Lactic acid is elevated in idiopathic pulmonary fibrosis and induces myofibroblast differentiation via pH-dependent activation of transforming growth factor- $\beta$ , *Am. J. Respir. Crit. Care Med.* 186 (2012) 740–751.
- [42] B. Faubert, K.Y. Li, L. Cai, C.T. Hensley, J. Kim, L.G. Zacharias, C. Yang, Q.N. Do, S. Doucette, D. Burguete, H. Li, G. Huet, Q. Yuan, T. Wigal, Y. Butt, M. Ni, J. Torrealba, D. Oliver, R.E. Lenkinski, C.R. Malloy, J.W. Wachsmann, J.D. Young, K. Kernstine, R.J. DeBerardinis, Lactate metabolism in human lung tumors, *Cell* 171 (2017) 358–371.e9.
- [43] H. Yu, J. Zhu, L. Chang, C. Liang, X. Li, W. Wang, 3-Bromopyruvate decreased kidney fibrosis and fibroblast activation by suppressing aerobic glycolysis in unilateral ureteral obstruction mice model, *Life Sci.* 272 (2021), 119206.
- [44] H. Ding, L. Jiang, J. Xu, F. Bai, Y. Zhou, Q. Yuan, J. Luo, K. Zen, J. Yang, Inhibiting aerobic glycolysis suppresses renal interstitial fibroblast activation and renal fibrosis, *Am. J. Physiol. Renal Physiol.* 313 (2017) F561–F575.
- [45] W. Qi, H.A. Keenan, Q. Li, A. Ishikado, A. Kannt, T. Sadowski, M.A. Yorek, I.-H. Wu, S. Lockhart, L.J. Coppey, A. Pfenninger, C.W. Liew, G. Qiang, A.M. Burkart, S. Hastings, D. Pober, C. Cahill, M.A. Niewczas, W.J. Israelsen, L. Tinsley, I.E. Stillman, P.S. Amenta, E.P. Feener, M.G. Vander Heiden, R.C. Stanton, G.L. King, Pyruvate kinase M2 activation may protect against the progression of diabetic glomerular pathology and mitochondrial dysfunction, *Nat. Med.* 23 (2017) 753–762.
- [46] M. Lee, G. Harley, M. Katerelos, K. Gleich, M.A. Sullivan, A. Laskowski, M. Coughlan, S.A. Fraser, P.F. Mount, D.A. Power, Mutation of regulatory phosphorylation sites in PFKFB2 worsens renal fibrosis, *Sci. Rep.* 10 (2020), 14531.
- [47] L. Wen, Y. Li, S. Li, X. Hu, Q. Wei, Z. Dong, Glucose metabolism in acute kidney injury and kidney repair, *Front. Med.* 8 (2021), 744122.
- [48] Y. Chen, L. Lin, X. Tao, Y. Song, J. Cui, J. Wan, The role of podocyte damage in the etiology of ischemia-reperfusion acute kidney injury and post-injury fibrosis, *BMC Nephrol.* 20 (1) (2019) 106, <https://doi.org/10.1186/s12882-019-1298-x>.
- [49] N.I. Skrypyuk, R.C. Harris, de M.P. Caestecker, Ischemia-reperfusion model of acute kidney injury and post injury fibrosis in mice, *J. Vis. Exp.* 78 (2013), 50495, <https://doi.org/10.3791/50495>.
- [50] N. Le Clef, A. Verhulst, P.C. D'Haese, B.A. Vervaeke, Unilateral renal ischemia-reperfusion as a robust model for acute to chronic kidney injury in mice, *PLoS One* 11 (2016), e0152153.
- [51] G.K. Reddy, C.S. Enwemeka, A simplified method for the analysis of hydroxyproline in biological tissues, *Clin. Biochem.* 29 (1996) 225–229.
- [52] J. Vandesompele, K. De Preter, F. Pattyn, B. Poppe, N. Van Roy, A. De Paepe, F. Speleman, Accurate normalization of real-time quantitative RT-PCR data by geometric averaging of multiple internal control genes, *Genome Biol.* 3 (2002). RESEARCH0034.
- [53] K. Yagi, Simple Assay for the Level of Total Lipid Peroxides in Serum or Plasma, *Free Radical and Antioxidant Protocols.* (n.d.) 101–106. <https://doi.org/10.1385/0-89603-472-0:101>.
- [54] T. Bücher, R. Czok, W. Lamprecht, E. Latzko, Pyruvate, *Methods of Enzymatic Analysis*, 1965, pp. 253–259, <https://doi.org/10.1016/b978-0-12-395630-9.50055-4>.
- [55] D. Johnson, Lardy, isolation of rat liver and kidney mitochondria, *Methods Enzymol.* 10 (1967) 94–101.
- [56] G.L. Peterson, Determination of total protein, *Methods Enzymol.* 91 (1983) 95–119.
- [57] M. Spinazzi, A. Casarin, V. Pertegato, L. Salvati, C. Angelini, Assessment of mitochondrial respiratory chain enzymatic activities on tissues and cultured cells, *Nat. Protoc.* 7 (2012) 1235–1246.
- [58] Isocitrate Dehydrogenase, in: *Methods of Enzymatic Analysis*, Elsevier, 1974, p. 624.
- [59] H. Bisswanger, *Practical Enzymology: BISSWANGER: PRACTICAL ENZYME 2 O-BK*, second ed., Wiley-VCH Verlag, Weinheim, Germany, 2011.
- [60] H. Tkachenko, N. Kurhaluk, T. Hetmański, A. Włodarkiewicz, V. Tomin, Changes in energetic metabolism and lysosomal destruction in the skeletal muscle and cardiac tissues of pigeons (*Columba livia f. urbana*) from urban areas of the northern Pomeranian region (Poland), *Ecotoxicology* 30 (2021) 1170–1185.
- [61] A. Allen, B. Friedmann, S. Weinhouse, Tissue preferences for fatty acid and glucose oxidation, *J. Biol. Chem.* 212 (1955) 921–933.

- [62] N. Yamamoto, M. Ueda-Wakagi, T. Sato, K. Kawasaki, K. Sawada, K. Kawabata, M. Akagawa, H. Ashida, Measurement of glucose uptake in cultured cells, *Curr. Protoc. Pharmacol.* 71 (2015), 12.14.1–12.14.26.
- [63] S.J. Pilkis, Glucokinase of rat liver, *Methods Enzymol.* 42 (1975) 31–39.
- [64] R.G. Kemp, Phosphofructokinase from rabbit skeletal muscle, *Methods Enzymol.* 42 (1975) 71–77.
- [65] J.M. Cardenas, Pyruvate kinase from bovine muscle and liver, *Methods Enzymol.* (1982) 140–149, 90 Pt E.
- [66] C.Y. Lee, J.H. Yuan, E. Goldberg, Lactate dehydrogenase isozymes from mouse, *Methods Enzymol.* (1982) 351–358, 89 Pt D.
- [67] J.A. Sibley, A.L. Lehninger, Determination of aldolase in animal tissues, *J. Biol. Chem.* 177 (1949) 859–872, [https://doi.org/10.1016/s0021-9258\(18\)57031-9](https://doi.org/10.1016/s0021-9258(18)57031-9).